# Triaxial shape induced by couplings between equatorial orbitals

Bao-Guo Dong,[1,2] Hong-Chao Guo,[1] and I. Ragnarsson[2]
[1]*Department of Nuclear Physics, China Institute of Atomic Energy, P.O. Box 275, Beijing 102413, China*
[2]*Division of Mathematical Physics, Lund Institute of Technology, P.O. Box 118, S-22100, Lund, Sweden*
(Received 8 December 2004; revised manuscript received 20 March 2006; published 13 July 2006)

The observed signature splitting at high spin in the odd-odd isotopes $^{126-132}$Pr and its description in cranking calculations suggest that $^{126}$Pr ($Z = 59$, $N = 67$) is triaxially deformed at intermediate values. The triaxial shape is explained as caused by specific couplings between the orbitals. These couplings are active for $N = 67$ but not for $N = 69$.

DOI: 10.1103/PhysRevC.74.014308 PACS number(s): 21.10.Hw, 21.10.Re, 21.60.Ev, 27.60.+j

## I. INTRODUCTION

It is an empirical fact that most nuclei are axially deformed in their ground states but it is also well established that triaxial shapes are realized at very high angular momenta, e.g., in the strongly deformed bands in Lu nuclei [1,2], in terminating bands when approaching the noncollective limit [3], or in the triaxial high-spin bands in $^{138-140}$Nd [4,5]. The possibility of triaxial shapes at low or intermediate spin values is, however, a more controversial issue. For spin values $I \lesssim 20$, it is especially the so-called signature inversion in rotational bands based on a high-$j$ proton and a high-$j$ neutron that has been presented as evidence for triaxial shape. In this article, we also consider these types of bands but at somewhat higher spin values in the $I = 20$–$30$ range, where no signature inversion is observed. Our analysis shows that the systematics of the signature splitting in $\pi h_{11/2}\nu h_{11/2}$ bands in odd-odd Pr nuclei suggest that triaxial shape is realized in rotational bands based on specific single-particle configurations.

Signature inversion [6] is observed at low spin in odd-odd nuclei with both of the odd particles in high-$j$ orbitals. It corresponds to an energy ordering between odd and even spin states that is different from what would be expected from general rules at axial symmetry and has been taken as evidence that these nuclei are triaxially deformed. However, this conclusion appears uncertain because the arguments [6] are in their most straightforward formulation based on the cranking model, which is difficult to justify at the small angular momenta in question( see e.g. Ref. [7] for a critical discussion). Furthermore, it turns out that the signature inversion might be explained by other terms not present in the simple estimates, e.g., by dynamical rather than static deformations in terms of vibrations [8] or wobbling [9], by the residual $pn$ interaction [10], or by quadrupole pairing interactions [11].

In view of the ambiguities at low spin values, we consider intermediate spins where the cranking model can be well justified. Specifically, we concentrate on the $I \sim 20$–$30$ states in the bands built on an $h_{11/2}$ proton and an $h_{11/2}$ neutron in the odd-odd $Z = 59$ Pr isotopes with $N = 67$–$73$. The evolution of the signature splitting in these bands shows an unexpected discontinuity when approaching the most deformed nuclei near the middle of the shell at $N = 66$. It turns out that standard cranking calculations with no fit of parameters describe this discontinuity although the deformation varies as expected, i.e., it increases with decreasing neutron number in the full range $N = 73$–$67$. A closer investigating reveals that the calculated discontinuity is caused by a transition to triaxial shape, i.e., although the energy minimum is calculated at $\gamma \approx 0^\circ$ in $^{128}$Pr, it is found at $\gamma \approx -10^\circ$ in $^{126}$Pr. Further analysis reveals that the transition to triaxial shape is caused by specific couplings between the equatorial single-particle orbitals. These couplings [12,13], which have been discussed previously in connection with fission barriers, have a specific dependence on particle number so that, essentially independent of parameters, there is a driving force toward triaxial shape for $N = 67$ but not for $N = 69$. These facts taken together make us conclude that the calculations give a correct description of the experimental data. Consequently, it appears that, in this specific configuration, $^{126}$Pr is triaxially deformed, whereas $^{128}$Pr is probably close to axial.

## II. GENERAL FEATURES OF HIGH-j CONFIGURATIONS

For an elementary understanding of the coupling scheme, we consider an odd-odd nucleus with the odd proton and odd neutron in orbitals with high angular momenta, $j_p$ and $j_n$, respectively. The Coriolis force tends to align these spin vectors at rapid rotation, i.e., they will give a spin contribution of almost $j_{pn} = j_p + j_n$. When combined with the "ground band" of the core with $I = 0, 2, 4, \ldots$, angular momenta with $I = j_{pn}, j_{pn} + 2, \ldots$ will be energetically favored over those with $I = j_{pn} + 1, j_{pn} + 3, \ldots$. These two bands are referred to as having different signature $\alpha = j_{pn} (\mathrm{mod}\ 2)$, i.e., $\alpha$ takes the values 0 or 1 in an odd-odd nucleus.

These simple arguments suggest that the favored signature band will always be lowest in energy at high spin and this is also what is observed experimentally. At lower spin values close to $j_{pn}$, however, the Coriolis force will be weak so different scenario might be realized. Morever, if one of the particles is in the middle of the $j$ shell, its signature splitting caused by the Coriolis force will be small and even close to vanishing. Therefore, small additional effects might even reverse the two signature bands so that the unfavored signature is lowest in energy in a limited spin range. Indeed, experimental observations indicate that this is a systematic feature occurring in different regions of the nuclear periodic table including the $N \approx 70$ Pr isotopes [14].

 

Different ways to describe the signature inversion have been suggested [6,8–11] but this description is achieved either by using some parameters whose values are uncertain or, in the case of $\gamma$ deformation, by using a model which is difficult to justify at the low spin values where signature inversion is observed [7]. This differs very much from our description of the data in Pr nuclei, which is achieved using the configuration-dependent Cranked Nilsson-Strutinsky (CNS) model [3,15], which has been extremely successful when describing experimental data (see e.g. Ref. [16]). Furthermore, our results are essentially independent of the parameters used. The different mechanisms discussed in connection with signature inversion might be active also at the somewhat higher spin values considered by us. However, they are rather small and they should vary smoothly with particle number. Thus, it is very unlikely that they can be invoked to explain the discontinuity observed for the Pr isotopes between $N = 67$ and 69.

The signature dependence of the orbitals in an $h_{11/2}$ shell at prolate and close-to-prolate shape is shown in Fig. 1. The favored $\alpha = -1/2$ branches of the orbitals are lowest in energy at high spin and far down in the shell but the two signature branches are almost degenerate at small rotational frequencies in the middle of the shell. Note that the dependence

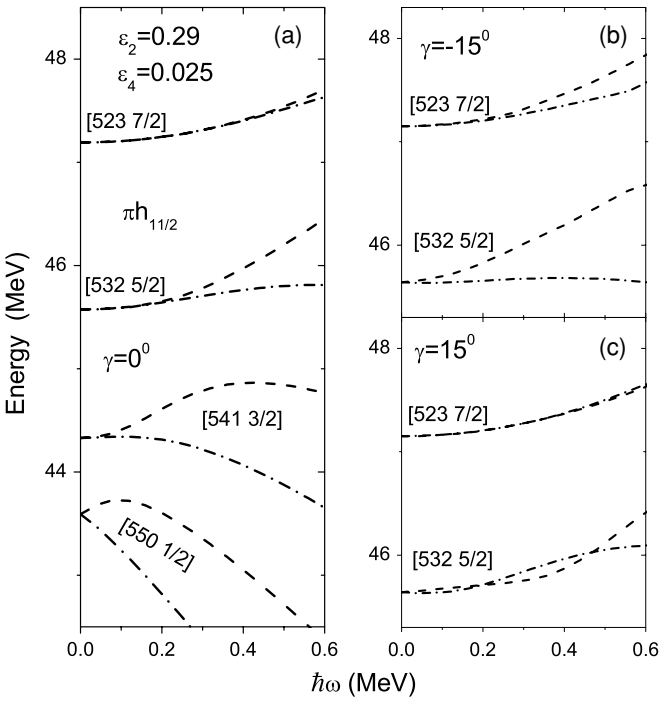


FIG. 1. Single-particle orbitals (Routhians) in the $h_{11/2}$ shell, labeled by the asymptotic quantum numbers, $[Nn_z\Lambda\Omega]$, drawn versus rotational frequency, $\omega$, at a fixed quadrupole deformation, $\varepsilon_2 = 0.29$. Axial shape is assumed in the panel to the left and triaxial shape with rotation around the intermediate ($\gamma = -15^\circ$) and the shorter ($\gamma = 15^\circ$) axis, respectively, in the two panels to the right where only the third and fourth orbitals are shown. Orbitals with signature $\alpha = +1/2$ and $-1/2$, respectively, are drawn by dashed and dot-dashed lines. Note that the signature splitting for these orbitals in the middle of the shell are strongly dependent on $\gamma$.

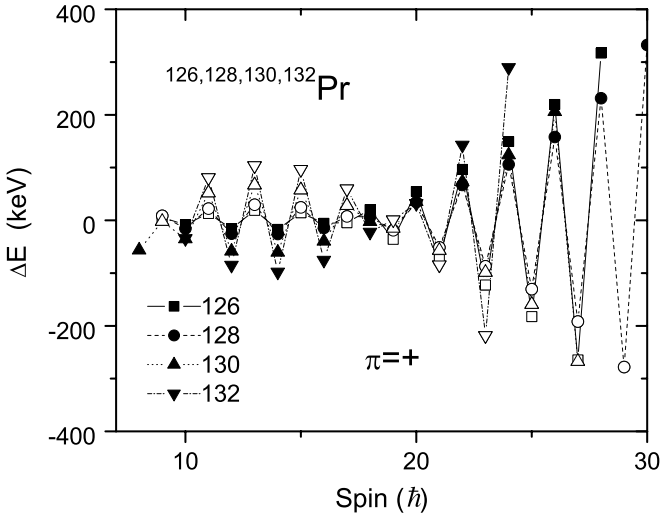


FIG. 2. Observed signature splittings in the odd-odd $Z = 59$ Pr isotopes with $N = 67$–73 for the rotational bands built on an odd $h_{11/2}$ proton and an odd $h_{11/2}$ neutron.

of the triaxiality parameter $\gamma$ is about equally strong for all $\omega$ values although it is only for low rotational frequencies that a signature inversion is calculated. Even so, the $\gamma$ dependence could as well be studied at somewhat higher $\omega$ values. The corresponding spin values are easier to treat theoretically because the spin direction is more well defined so the cranking approximation becomes more reliable. Furthermore, pairing is strongly quenched. Therefore, more safe conclusions about the origin of the disturbances might be reached at high spin values.

## III. SIGNATURE SPLITTING IN THE $\pi h_{11/2}\,\nu h_{11/2}$ BANDS OF $^{126-132}$Pr

When considering the signature splitting, we use the same quantity as in Ref. [14], namely

$$\Delta E(I) = E(I) - E(I-1) - \frac{E(I+1) - E(I) + E(I-1) - E(I-2)}{2}. \quad (1)$$

This quantity is plotted for the observed $\pi h_{11/2}\nu h_{11/2}$ bands of $^{126-132}$Pr in Fig. 2. It is evident that all the bands show similar features with a small signature inversion (favoring of the even spin states) for $I = 10$–18, but, as expected from the discussion above, an increasing *Coriolis splitting* for spin values beyond $I = 20$, i.e., a lowering of those (odd spin) states favored by the Coriolis force.

There is a general effect that the deformation becomes largest in the middle between closed shells, i.e., around $N = 66$ for the Pr isotopes. In the present case, one would thus expect that the deformation increases with decreasing neutron number toward $N = 66$, i.e., in the whole range, $N = 73$–67. This is what comes out from the present calculations (see Fig. 5 below) and similar results are obtained in the folded Yukawa calculations of Ref. [17]. As a consequence of the increasing deformation, the Coriolis force becomes less effective because those orbitals that couple through the Coriolis

Hamiltonian are split further apart (see e.g. Ref. [18]). These expectations are consistent with the trends at high spin for $N = 73$–$69$ shown in Fig. 2, where the Coriolis splitting at high spin decreases with decreasing neutron number. The trend is however broken for the lowest neutron number, i.e., the Coriolis splitting is larger in the $N = 67$ nucleus $^{126}$Pr than in the $N = 69$ nucleus $^{128}$Pr. This is thus unexpected from the simple arguments based on increasing deformation but, as we shown below, it can be understood if deformations breaking the axial symmetry are also accounted for. Note also that even though the discontinuity might seem rather small, it is about *as large as the maximum amplitude in the signature inversion region*, $I = 10$–$16$.

The trend of the Coriolis splitting relies on the spin assignments and most spin values are not fixed from experiment but rather from general features of the transition energies when considered as functions of particle number. We have thus used the spin assignments from Liu *et al.* [19] that have been extended to lower neutron numbers by Hartley *et al.* [20]. They lead to the smooth trends shown in Fig. 7 of that reference. We have also tested these spin values according to the methods of Ref. [21], where absolute energies are normalized to measured masses, making it possible to compare also with the odd Pr neighbors at high spin where pairing is negligible. These comparisons lead to large discontinuities if other spin values than those of Ref. [14] are used, making us fully convinced that these spin assignments are correct.

## IV. CONFIGURATION DEPENDENT CRANKING CALCULATIONS ON $^{126-132}$Pr

We have carried out calculations for the $\pi h_{11/2}\nu h_{11/2}$ bands in $^{126-132}$Pr using the CNS approach [3,15]. Pairing is neglected in this formalism and the different configurations are described by the number of particles in the different $N$ shells and how they are distributed between the high-$j$ intruder shells and the other subshells, respectively. The proton configuration of these $Z = 59$ bands are described as having six of the valence protons in orbitals of $d_{5/2}$, $g_{7/2}$ character and three in $h_{11/2}$ orbitals. The odd $h_{11/2}$ proton will then be placed in the favored $\alpha = -1/2$ branch of the [541 3/2] orbital, with the $\alpha = 1/2$ branch too high in energy (see Fig. 1) to become occupied in the observed bands. The most important negative parity neutron configuration will have seven valence particles in $h_{11/2}$ orbitals where the odd neutron in the [523 7/2] orbital will determine the observed signature splitting. The other valence neutrons outside the $N = 50$ gap will occupy the $N = 4$ orbitals. In the CNS formalism all valence particles in the different groups of orbitals are specified, i.e., the configurations assigned to the observed bands in $^{126-132}$Pr are labeled $\pi(h_{11/2})^3\nu(h_{11/2})^7$. The number of particles in the $N = 4$ valence shells is then fixed to get the correct number of protons and neutrons (in the shorthand notation that is generally used; see e.g. Ref. [3], these configurations would be labeled [03,7] where, in addition to the $h_{11/2}$ particles, it is also specified that there are no holes in the $g_{9/2}$ proton orbitals).

The calculated $\pi(h_{11/2})^3\nu(h_{11/2})^7$ bands are compared with the observed $\pi h_{11/2}\nu h_{11/2}$ bands (where only the odd high-$j$ particles are specified) in Fig. 3. The bands are shown relative

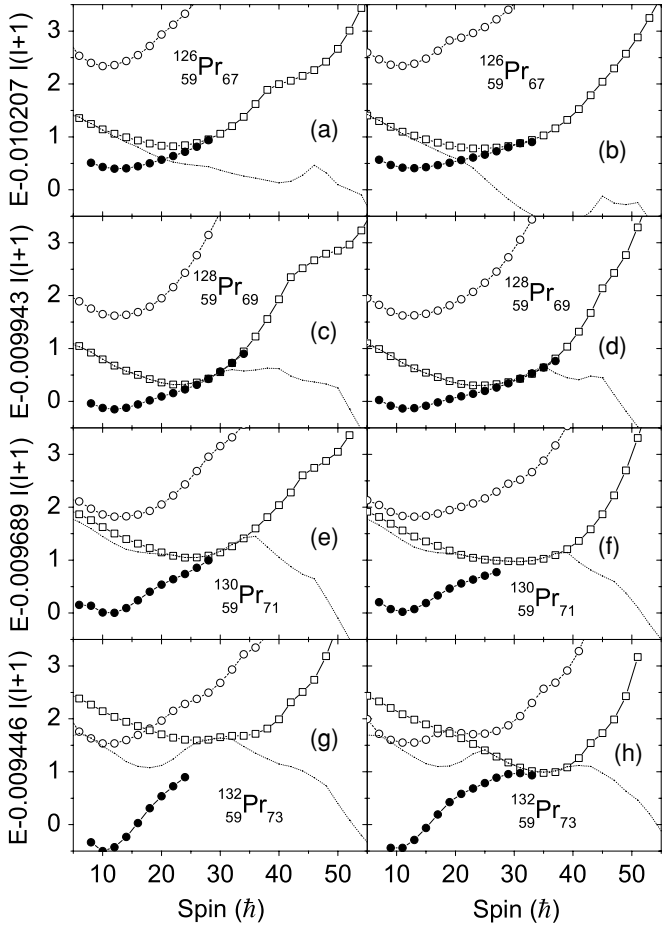


FIG. 3. Total energy (MeV) versus spin for positive parity bands of both signatures (left $\alpha = 0$ and right $\alpha = 1$) in $^{126-132}$Pr. The energies are given relative to a rigid rotation reference $(\hbar^2/2J_{\rm rig})I(I+1)$ as defined in Ref. [3]. The calculated yrast lines are indicated by dotted lines. The open symbols indicate the theoretical data [circle $\pi(h_{11/2})^1\nu(h_{11/2})^7$ and square $\pi(h_{11/2})^3\nu(h_{11/2})^7$] and solid symbols the experimental data.

to a rigid rotation reference. At low spin and small deformation, the $\pi(h_{11/2})^1\nu(h_{11/2})^7$ bands come low in energy so they are also shown in Fig. 3. Because of the neglect of pairing, the present calculation will only give a qualitative description at low-spin values but they should become realistic at higher spin values, say $I > 20\hbar$. Therefore, the calculated bands are normalized to the observed ones at the highest spin values in Fig. 3. In those cases where the bands are observed far beyond $I = 20$ there is a very good correspondence between experiment and calculations in the high-spin region giving further confidence to the present calculations. Note also that for high spin values in the lighter isotopes, the $\pi(h_{11/2})^3\nu(h_{11/2})^7$ bands are not calculated as yrast. Even so, considering the good agreement between calculations and experiment, it appears safe to assign the $\pi(h_{11/2})^3\nu(h_{11/2})^7$ configuration to all these bands. For example, the $\pi(h_{11/2})^3\nu(h_{11/2})^5$ configuration leads to a much too large signature splitting with no correspondence in the observed bands. The assignment of the $\pi(h_{11/2})^3\nu(h_{11/2})^7$ configuration to the signature-split band even in the lightest isotope, $^{126}$Pr, is also supported by the fact that the ground-state

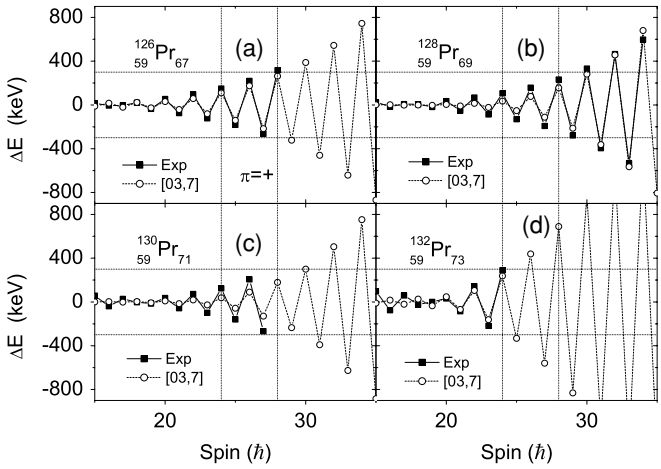


FIG. 4. Energy staggering $\Delta E(I)$ as defined in Eq. (1) plotted versus spin for the $\pi h_{11/2}\nu h_{11/2}$ bands in $^{126-132}$Pr. Open symbols indicate theoretical data for the configuration $\pi(h_{11/2})^3\nu(h_{11/2})^7$ and solid symbols experimental data [14]. A signature splitting of $\delta E$ for the relevant orbital in Fig. 1 will roughly correspond to an amplitude of $4\Delta E$ with our definition of $\Delta E$, see Eq. (1). Thin lines at fixed spins and energies are drawn to facilitate the comparison between the different isotopes.

band head in the neighbor isotone, $^{125}$Ce, has been assigned [22] as built on the same neutron orbital, i.e., the seventh $h_{11/2}$ orbital, [523 7/2].

The close correspondence between calculations and experiment is further accentuated in Fig. 4 where observed and calculated signature splittings are compared. The observed trends at high spin discussed above are clearly reproduced by the calculations, especially the fact that the splitting is larger for $^{126}$Pr than for $^{128}$Pr although $^{126}$Pr is calculated to be more deformed. It turns out that the calculated larger splitting in $^{126}$Pr is caused by triaxial deformation with $\gamma \approx -10^\circ$, i.e., rotation around the intermediate principal axis. This is illustrated in Fig. 5 where the deformation trajectories for the $\pi(h_{11/2})^3\nu(h_{11/2})^7$ configurations are shown. Note that this minimum is clearly located at negative $\gamma$ values so that even if one would expect dynamical fluctuations around this equilibrium, the average value of $\gamma$ will remain negative. This is contrary to the ground state where there is an exact (even-even nuclei) or approximate (odd and odd-odd nuclei) symmetry around $\gamma = 0^\circ$, so that dynamical fluctuations might result in an average $\gamma$ value that is zero.

A substantial triaxial deformation is also calculated for odd spins in $^{132}$Pr. However, no specific trend in the observed signature splitting supports this observation and therefore it is discussed no further. One may, however, note that this nucleus is on the borderline of the region where chiral bands, giving evidence for triaxial deformation, have been reported, see e.g., Ref. [23].

## V. SINGLE-PARTICLE EFFECTS CAUSING TRIAXIAL DEFORMATION

A further question is if it is possible to get a deeper understanding why $^{126}$Pr is triaxially deformed but $^{128}$Pr is not.

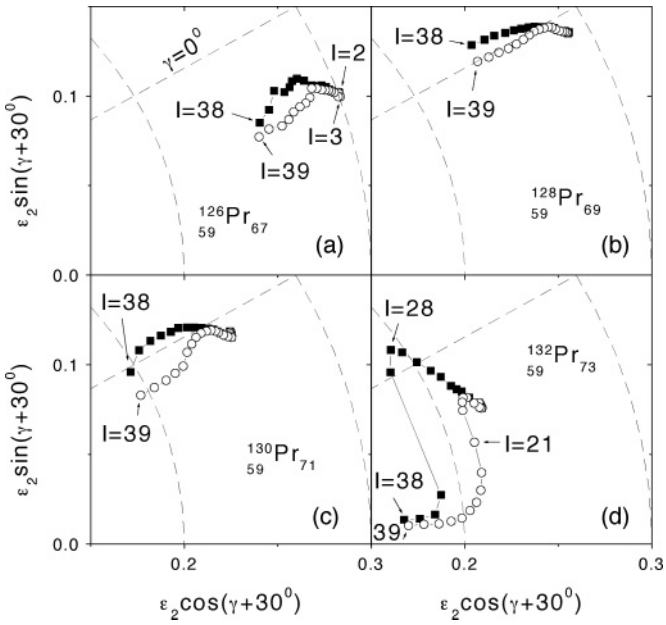


FIG. 5. Deformation trajectories in the $(\varepsilon_2, \gamma)$ plane for the calculated $\pi(h_{11/2})^3\nu(h_{11/2})^7$ configurations of $^{126-132}$Pr.

For this purpose, the single-particle Routhians are drawn in Fig. 6 as a function of the axial asymmetry parameter, $\gamma$. This figure gives a good understanding of the difference between the two isotopes and indicates that the triaxiality in $^{126}$Pr is caused by two effects that have been discussed previously but that have not been confirmed from spectroscopic data.

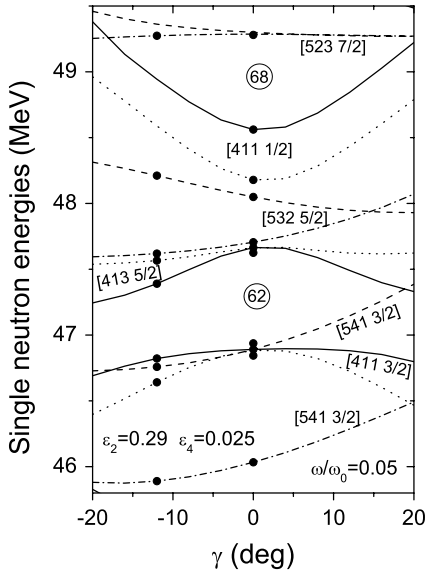


FIG. 6. Calculated single-neutron Routhians labeled by $[Nn_z\Lambda\Omega]$ shown versus the triaxiality parameter $\gamma$ with fixed values of the other deformation parameters ($\varepsilon_2 = 0.29$, $\varepsilon_4 = 0.025$) and the rotational frequency ($\omega/\omega_0 = 0.05$). The $N = 5h_{11/2}$ orbitals are drawn by dot-dashed ($\alpha = -1/2$) and dashed ($\alpha = +1/2$) lines and the $N = 4$ orbitals by dotted ($\alpha = -1/2$) and full ($\alpha = +1/2$) lines. The orbitals filled in the $\nu(h_{11/2})^7$ configuration for $N = 67$ and 69 are indicated at $\gamma = -12^\circ$ and $\gamma = 0^\circ$, respectively.

First, it was realized in Ref. [24] that with a high-$j$ shell filled to $\approx$ 25%–50%, i.e., for 3–7 particles in $h_{11/2}$, these particles will drive the nucleus toward negative values of $\gamma$ for the intermediate spin values discussed here. The trend toward negative $\gamma$ for the third, fourth, and fifth $h_{11/2}$ orbital, [541 3/2], $\alpha = \pm 1/2$ and [532 5/2], $\alpha = -1/2$, is clearly seen in Fig. 6. Thus, there is a driving force toward negative $\gamma$ both for the 3 $h_{11/2}$ protons and for the 7 $h_{11/2}$ neutrons. This trend is not very strong but if supported by the other particles it might overcome the forces trying to preserve the axially symmetric shape.

The second driving force toward triaxial shape is different for $N = 67$ and 69. In general, it is caused by couplings within orbitals having asymptotic quantum numbers with $n_z = 1$ or 0, i.e., the orbitals located at the equator of the nucleus. Such couplings have previously been discussed [12,13] in connection with triaxial shapes when a nucleus traverses a fission barrier. For the Pr isotopes, the important couplings are between the $N = 4, n_z = 1$ neutron orbitals. Three orbitals of that kind, [411 3/2], [413 5/2], and [411 1/2], come close together in the vicinity of the neutron Fermi surface as indicated in Fig. 6. Because they interact strongly through the operator describing triaxial shape, $r^2(Y_{22} + Y_{2-2})$ [12,13], the lower ones will bend downward and the higher ones will bend upward with increasing triaxial shape. Consequently, if only the lower ones of these orbitals are filled, they will give a driving force toward triaxiality. This is indeed the case for the $\nu(h_{11/2})^7$ configuration of $^{126}$Pr. However, $^{128}$Pr, they are all filled which means that there is no special tendency toward triaxiality. This difference between $^{126}$Pr and $^{128}$Pr is quite large and easily visible in the calculated potential energy surfaces that are much softer in the $\gamma$ direction for $^{126}$Pr than for $^{128}$Pr. For example, if $\gamma$ is varied by $\pm 20^\circ$ around the minimum, the energy will reach only values that are approximately 0.6 MeV above the minimum in $^{126}$Pr, whereas the energy comes more than 1.6 MeV above the minimum for $^{128}$Pr. If this softness toward nonaxial shape is combined with the general tendency toward negative $\gamma$ values, it leads to triaxial shapes in $^{126}$Pr although the energy surface is too stiff in $^{128}$Pr to move the minimum away from $\gamma = 0^\circ$. Note that the difference between $^{126}$Pr and $^{128}$Pr is essentially independent of parameters because with seven valence neutrons in $h_{11/2}$ orbitals, all three $N = 4, n_z = 1$ neutron orbitals must be occupied for $N = 69$, whereas only two of them are occupied for $N = 67$. It is also important that the pairing correlations are weak because large pairing correlations would lead to a partial occupation of the different orbitals.

## VI. SUMMARY

The signature splitting at high spin values of the $\pi h_{11/2} \nu h_{11/2}$ bands in the odd-odd $^{126-132}$Pr isotopes are well reproduced by cranking calculations using the modified oscillator potential. The trend of decreasing signature splitting with decreasing neutron number is broken by $^{126}$Pr supporting the calculated triaxial deformation for this nucleus. The triaxial deformation is caused by specific couplings between the single-particle orbitals that are active for $N = 67$ but not for $N = 69$.

## ACKNOWLEDGMENTS

This work is supported by the National Natural Science Foundation of China under Grant No. 10275093, by the Swedish Science Research Council, and by the Crafoord Foundation.

[1] S. W. Ødegård, G. B. Hagemann, D. R. Jensen, M. Bergström, B. Herskind, G. Sletten, S. Törmänen, J. N. Wilson, P. O. Tjøm, I. Hamamoto, K. Spohr, H. Hübel, A. Görgen, G. Schönwasser, A. Bracco, S. Leoni, A. Maj, C. M. Petrache, P. Bednarczyk, and D. Curien, Phys. Rev. Lett. **86**, 5866 (2001).
[2] G. B. Hagemann, Eur. Phys. J. A **20**, 183 (2004).
[3] A. V. Afanasjev, D. B. Fossan, G. J. Lane, and I. Ragnarsson, Phys. Rep. **322**, 1 (1999).
[4] C. M. Petrache, G. LoBianco, D. Ward, A. Galindo-Uribarri, P. Spolaore, D. Bazzacco, T. Kröll, S. Lunardi, R. Menegazzo, C. Rossi Alvarez, A. O. Macchiavelli, M. Cromaz, P. Fallon, G. J. Lane, W. Gast, R. M. Lieder, G. Falconi, A. V. Afanasjev, and I. Ragnarsson, Phys. Rev. C **61**, 011305(R) (2000).
[5] C. M. Petrache, M. Fantuzi, G. LoBianco, D. Mengoni, A. Neusser-Neffgen, H. Hübel, A. Al-Khatib, P. Bringel, A. Bürger, N. Nenoff, G. Schönwasser, A. K. Singh, I. Ragnarsson, G. B. Hagemann, B. Herskind, D. R. Jensen, G. Sletten, P. Fallon, A. Görgen, P. Bednarczyk, D. Curien, G. Gangopadhyay, A. Korichi, A. Lopez-Martens, B. V. T. Rao, T. S. Reddy, and N. Singh, Phys. Rev. C **72**, 064318 (2005).
[6] R. Bengtsson, H. Frisk, F. R. May, and J. A. Pinston, Nucl. Phys. **A415**, 189 (1984).
[7] I. Hamamoto, Nucl. Phys. **A520**, 297c (1990).
[8] A. Ikeda and T. Shimano, Phys. Rev. C **42**, 149 (1990).
[9] M. Matsuzaki, Phys. Rev. C **46**, 1548 (1992).
[10] P. B. Semmes and I. Ragnarsson, Proceedings of Future Directions in Nuclear Physics with $4\pi$ Gamma Detection Systems of the New Generation, Strasbourg, March 1991, edited by J. Dudek and B. Haas (AIP Conf. Proc. 259, 1992) p. 566; Proceedings of the International Conference on High-Spin Physics and Gamma-Soft Nuclei, Pittsburgh, September 1990, edited by J. X. Saladin, R. A. Sorensen, and C. M. Vincent (World Scientific, Singapore, 1991), p. 500.
[11] F. R. Xu, W. Satula, and R. Wyss, Nucl. Phys. **A669**, 119(2000).
[12] S. E. Larsson, P. Möller, and S. G. Nilsson, Phys. Scr. **A10**, 53 (1974).
[13] I. Ragnarsson, S. G. Nilsson, and R. K. Sheline, Phys. Rep. **45**, 1 (1978).
[14] D. J. Hartley, A. Galindo-Uribarri, C. Baktash, M. P. Carpenter, M. Danchev, M. Devlin, C. J. Gross, R. V. F. Janssens, M. Lipoglavsek, E. Padilla, S. D. Paul, D. C. Radford, W. Reviol, L. L. Riedinger, D. G. Sarantites, D. Seweryniak, C.-H. Yu, and O. Zeidan, Phys. Rev. C **63**, 041301(R) (2001).
[15] T. Bengtsson and I. Ragnarsson, Nucl. Phys. **A436**, 14 (1985).
[16] W. Satula and R. A. Wyss, Rep. Prog. Phys. **68**, 131 (2005).

[17] P. Möller, J. R. Nix, W. D. Myers, and W. J. Swiatecki, At. Data Nucl. Data Tables **59**, 185 (1995).
[18] S. G. Nilsson and I. Ragnarsson, *Shapes and Shells in Nuclear Structure* (Cambridge University Press, Cambridge, 1995).
[19] Y. Liu, J. Lu, Y. Ma, S. Zhou, and H. Zheng, Phys. Rev. C **54**, 719 (1996).
[20] D. J. Hartley *et al*., Phys. Rev. C **65**, 044329 (2002).
[21] I. Ragnarsson, F. G. Kondev, E. S. Paul, M. A. Riley, and J. Simpson, Int. J. Mod. Phys. E **13**, 87 (2004).
[22] C. M. Petrache, G. Lo Bianco, P. G. Bizzeti, A. M. Bizetti-Sona, D. Bazzacco, S. Lunardi, M. Nespolo, G. de Angelis, P. Spolaore, N. Blasi, S. Brant, V. Krstić, and D. Vretenar, Eur. Phys. J. A **14**, 439 (2002).
[23] S. Frauendorf, Rev. Mod. Phys. **73**, 463 (2001).
[24] G. Andersson, S. E. Larsson, G. Leander, P. Möller, S. G. Nilsson, I. Ragnarsson, S. Åberg, R. Bengtsson, J. Dudek, B. Nerlo-Pomorska, K. Pomorski, and Z. Szymański, Nucl. Phys. **A268**, 205 (1976).